Annex A: Mesh, SST k-ω and ANSYS simulations.

This section offers a deeper insight of the importance of the Meshing process during the elaboration of this project and the Shear Stress Transport k-ω model (SST)

Meshing process.

The process for generating a mesh of nodes and elements consists of three general steps:

1. Set the element attributes.
2. Set the mesh control.
3. Meshing the model.

It is not always necessary to set mesh controls because default mesh controls are appropriate for many models. If no controls are specified, the program will use the default settings to produce a free mesh. Alternatively, the SmartSize feature can be used to produce a better quality free mesh.

Also, the default mesh controls that ANSYS program uses may produce a mesh that is adequate for each model that is being analyzed. Mesh controls allow to establish such factors as element shape or element size.[(3)], and it offers more control over the mesh too.

When generating the mesh for this particular project, it was essential to find a balanced situation between a dense mesh and a light one. The more accurate the mesh was, the more time would be recquired. Without overlooking the relevance of a good mesh, a meshig process that recquired too much time would have been counterproductive. Therefore, the desired equilibrium between velocity and pressure lied in selecting the adequeate mixture

of a dense mesh and a lighter one.

- **Dense mesh:** the main advantage of a very dense mesh was that it offered a great accurancy in terms of calculation and results. However, it could take a very long time to obtain the final results, and this sluggish process could even block the computer or not reach a converged result.
- **Light mesh:** a lighter mesh can display the final results in an almost instantaneous way. However, these could probably differ very much from the reality, and they would be very far from the accurancy given by a more dense mesh.

Therefore, the mesh that was considered to be most suitable for this project was the one whose residual results were smaller that $1 \cdot 10^{-3}$.Given that the design into which this project focuses is a 3D object, the complete mesh does not need to be particularly small and precise, but only certain parts of the geometry. A posterior refinement was executed, so that the results may be more accurate and realistic

Therefore, it is stated that the importance of stablishing the correct mesh is unquestionable. As a consequence, many parameters must be taken care of in order to set reach the perfect configuration.

Mesh Control overview.

Physics preference.

The physics preference option allows establishing how ANSYS will perfom meshing based on the physics of the analysis type that has been specified. The available options are: Mechanical, Electromagnetic, CFD and Explicit. For this particular project, the suitable configuration is CFD.

Figure 1 depicts some of the physics preferences for the current case. The highlighted section shows the configuration for the CFD option.

Meshing Control	Physics Preference						
	Mechanical		Electro-magnet-ic	CFD			Explicit
	Mechanic-al APDL Solver	Rigid Body Dy-namics Solver		CFX-Solv-er	Fluent-Solver	Polyflow Solver	
Relevance Cen-ter (p. 76)	Coarse	Coarse	Medium	Coarse	Coarse	Coarse	Medium
Element Size (p. 77)	Default	Default	Default	Default	Default	Default	Default
Initial Size Seed (p. 77)	Active As-sembly	Active As-sembly	Active As-sembly	Active As-sembly	Active As-sembly	Active As-sembly	Active As-sembly
Smooth-ing (p. 77)	Medium	Medium	Medium	Medium	Medium	Medium	High
Trans-ition (p. 78)	Fast	Fast	Fast	Slow	Slow	Slow	Slow
Span Angle Cen-ter (p. 78)	Coarse	Coarse	Coarse	Fine	Fine	Fine	Coarse

Figure 1. Physics Preference.

Relevance Center.

Relevance Center sets the gauge of the Relevance slider control in the Default group. Options are Coarse, Medium and Fine. The Default value, however, can be set automatically according to the Physics Preference setting. In this particular case, as Figure 1 depicts, it was advisable to set Relevance Center as Coarse, which is the default option in ANSYS Fluent.

Element Size.

Element Size allows specifying the element size used for the entire model. This seize can be used for all edge, face and body meshing. Still, as it will later be explained, there is the possibility of refinng these zones if they hold a special interest. In this particular case, given the fact that fluid analyses

require high accuracy, both body and edge mesh were refined individually.

Smoothing.

Smoothing attempts to improve element quality by moving locations of nodes with respect to surrounding nodes and elements. The Low, Medium or High option controls the number of smoothing iterations. In this particular case, smoothing was set High in order to obtain the maxium accuracy.

Transition.

Transition affects the rate at which adjacent elements will grow. Slow produces smooth transitions, while Fast produces more abrupt transitions. In the current project, Transitions was set Slow.

Span Angle Center.

Span Angel Center sets the goal for curvature based refinement. The mesh will subdivide in curved regions until the individual elements span this angle. The available options are Coarse, Medium and Fine. According to the need of high accuracy, Span Angle Center was set Fine.

Local Mesh Controls.

Local Mesh Controls are available when a Mesh object in the tree is highlighted and a tool from either the Mesh Control drop-down menu, or from first choosing Inser in the context menu is selected. However, the first thing to do is to select the desired element from the geometry and create a Named Selection.

Now, when generating the mesh for this project, it was considered that the body, faces and edges that were to be thoroughly studied had to present a more precise mesh. Therefore, it was decided to use

the Sizing Control option, so that those sections that required higher accuracy could be meshed individually.

Sizing Control.

The Sizing Control sets:

- The element size for a selected body, face or edge.
- The number of divisions along an edge.
- The element size within a user-defined "sphere of influence" [(3)] that can induce a selected body, face, edge or vertex.
- The element size within a user-defined "body of influence"[(3)].
- The minimum mesh sizing used for a selected body, face or edge. Furthermore, this setting overrides the default global sizing.

The basic steps for using the local Sizing control are:

1. Select the body, face, edge or vertex.
2. From the Mesh Control toolbar, choose Sizing (or right-click and choose Insert>Sizing).
3. Specify the options under Details of Sizing in the Type field.

Defining Local Mesh Sizing on a Body and Local Mesh Sizing on an Edge.

Figure 2 provides an overview of how to define local mesh sizing on a body and an edge.

1. Specify Type.	2. Specify Behavior.	3. Specify values for the applicable options. Applicable options are dependent on the settings of Behavior and Use Advanced Size Function (p. 68).
Element Size	• Soft • Hard	• Element Size • Growth Rate • Curvature Normal Angle • Local Min Size
Sphere of Influence	N/A	• Sphere Center • Sphere Radius • Element Size
Body of Influence	N/A	• Element Size • Growth Rate

Figure 2. Example of how to local mesh sizing on a body ora n edge.

Element Size.

If body, face or edge are selected, Element Size is one of the availabel options in the Type field. It is mandatory to enter a positive value in this field. Smaller values will generate more divisions, therefore building a more precise mesh. In this case, element size was used when setting the configuration for a local mesh sizing of hte body.

Number of divisions.

Number of divisions can be used with all mesherss. If an edge is selected, the options available in the Type field are Element Size and Sphere of Influence, along with the Number of Divisions option. Choosing Number of Divisions and entering a value in the Number of Divisions field is an alternative to choosing Element Size. In this particular case, the Element Size was used when setting the configuration for the local mesh sizing of the edgesm and it was set at 500.

Shear Stress Transport k-ω model (SST).

Overview.

The starting point for the development of the SST model was the need for the accurate prediction of aerodynamics flows with strong adverse pressure gradients and separation. Over decades[1] the available turbulence models had consistently failed to compute these flows. In particular, the k-ε model was not able to capture the proper behavior of turbulent boundary layers up to separation. Nevertheless, the k-ω model is substantially more accurate than the k-ε in the near wall layers, and has therefore been successful for flows with moderate adverse pressure gradients, but fales for flows with pressure induced separation. In addition, the ω-equation shows a strong sensitivity to the values of ω in the freestream outside the boundary layer. This has largely prevented the ω-equation from replacing the ε-equation outside as the standard scale-equation in turbulence modelling, despite its superior performance in the near wall models.

Therefore, the shear stress transport (SST) k-ω model was developed by Menter[1] to effectively blend the robust and accurate formulation of the *k-ω* model in the near-wall region with the freestream independence of the *k-ε* model in the far field. To achieve this, the *k-ε* model was converted into a *k-ω* formulation. As a consequence, the SST *k-ω* model is similar to the standard *k-ω* model, but includes the following refinements:

- The standars *k-ω* model and the transformed *k-ε* model are both multiplied by a blending function and both models are added together. The blending function is designed to be one in the near-wall region, which activates the standard *k-ω* model, and zero away surface, which activated the *k-ε* model.

- The SST model incorporates a damped cross.diffusion derivative term in the *ω* equation.

- The definition of the turbulent viscosity is modified to account for the transport of the turbulent shear stress.

- The modelling constants are different.

These features make the SST *k-ω* model more accurate and reliable for a winder class of flows (for example, adverse pressure gradient flows, airfoils, etc.)[(2)].

Transport Equations for the SST *k-ω* Model.

The SST *k-ω* model has a similar form to the standard *k-ω* model:

$$\frac{\partial}{\partial t}(\rho k)+\frac{\partial}{\partial x_i}(\rho k u_i)=\frac{\partial}{\partial x_j}\left(\Gamma_k \frac{\partial k}{\partial x_j}\right)+G_k-Y_k+S_k$$

and

$$\frac{\partial}{\partial t}(\rho \omega)+\frac{\partial}{\partial x_j}\left(\rho \omega u_j\right)=\frac{\partial}{\partial x_j}\left(\Gamma_\omega \frac{\partial \omega}{\partial x_j}\right)+G_\omega-Y_\omega+D_\omega+S_\omega$$

Figure 3. Transport equations for the SST k-ω model.

In these equations, the term G_k represents the production of turbulence kinetic energy, Γ_k and Γ_ω represent the effective diffusivity of *k* and *ω*, Y_k and Y_ω represent the dissipation of *k* and *ω* due to turbulence, D_ω represents the corss-difusion term, and S_k and S_ω are user defined source terms.

Modelling the Effective Diffustivity.

The effective diffusivities for the SST *k-ω* model are given by Figure 2.

$$\Gamma_k=\mu+\frac{\mu_t}{\sigma_k}$$

$$\Gamma_\omega=\mu+\frac{\mu_t}{\sigma_\omega}$$

Figure 4. Effective diffusivities.

Where σk and σω are the turbulent Prandtl number for *k* and *ω*, respectively. The turbulence viscosity is computed as Figure 3 depicts.

$$\mu_t = \frac{\rho k}{\omega} \frac{1}{\max\left[\frac{1}{\alpha^*}, \frac{SF_2}{a_1 \omega}\right]}$$

Figure 5. Turbulence viscosity

With:

$$\sigma_k = \frac{1}{F_1/\sigma_{k,1} + (1 - F_1)/\sigma_{k,2}}$$

$$\sigma_\omega = \frac{1}{F_1/\sigma_{\omega,1} + (1 - F_1)/\sigma_{\omega,2}}$$

Figure 6. Strain rate magnitude.

Modeling the Turbulence Production.

Production of k.

The term Gk represents the production of turbulence kinetic energy, and is defines in the same manner as in the standard *k*-*ω* model [(2)].

Production of ω.

The term Gω represents the production of ω and is given by Figure 5.

$$G_\omega = \frac{\alpha}{\nu_t} G_k$$

Figure 7. Production of ω.

Modeling the Turbulence Dissipation.

Dissipation of k.

The term Yk represents the dissipation of turbulende kinetic energy, and is defined in a similar manner as in the standard *k-ω* model[(2)].

Dissipation of ω.

The term Yw represents the dissipation of ω, and is defined in a similar manner as in the standard *k-ω* model. The difference is in the way that some terms are evaluated. For instance, in the standard *k-ω* model, βi are defined as constant, while in the SST *k-ω* model it is given by Figure 6.

$$\beta_i = F_1 \beta_{i,1} + (1 - F_1)\beta_{i,2}$$

Figure 8. β term expressed as a non-constant value.

Wall Boundary Conditions.

The wall boundary conditions for the *k* equation in the *k-ω* models are treated in the same way as the *k* equation is treated when enhanced wall treatments are used with the *k-ε* models. This means that all boundary conditions for wall-function meshes will correspond to the wall function approach, while for the fine meshes, the appropriate low-Reynolds number boundary conditions will be applied.

Therefore, a wall treatment can be defined for the ω-equation, which switches automatically from the viscous sublayer formulation to the wall function, depending on the grid. This improved blending is the default behavior for near wall treatment.

ANSYS Simulations.

The central task in the natural science lies in describing reality as accurately as possible in order to better understand natural phenomena, and thus gain insight into the behavior of objects under given conditions.

Besides the practical and theoretical approaches, numerical simulation has established itself in recent years as a third approach whose user friendly nature and its relatively low cost has contributed to its popularity. While there are many numerical simulators for aerodynamic/hydrodynamic studies, ANSYS Fluent provides comprehensive capabilities for a wide range of options and fluids. In addition, the fact that it is installed and free to use in the facilities of ETSEIB, makes it even more accessible.

Bearing in mind the academic nature of this project, it is essential to state that the available economic resources are quite limited, thus complicating the physical construction of a model of a windsurfing board and its correspondent hydrofoil. Therefore, a perfect way to fully understand the behavior of water flow around the hydrofoil was to simulate the model with ANSYS. However, it is essential to remark that not every single simulation that has been executed appears in this Annex since, in most cases, the erroneous nature of the design was detected during the iteration process – while observing both the lift and drag coefficient Convergence History – which consequently led to the interruption of the iteration, so that a proper correction could be done and a new simulation could be carried out as soon as possible. Such is the case, for instance, of the Endplate winglet model, whose suspicious lift coefficient convergence history forced to repeatedly modify the design. The final result that appears detailed in this project was the latest version, which was executed right before reaching the conclusion that the blended winglet with bias tip was the adequate model to use.

Dismissed geometries: Elliptical model and Endplate model.

The elliptical model engendered some difficulties during the meshing process. Due to its highly curved sections, the geometry of the mesh seemed not to be able to adjust to the shape, thus complicating the process. As a consequence, it was necessary to modify the geometry several times, but no satisfactory results were obtained.

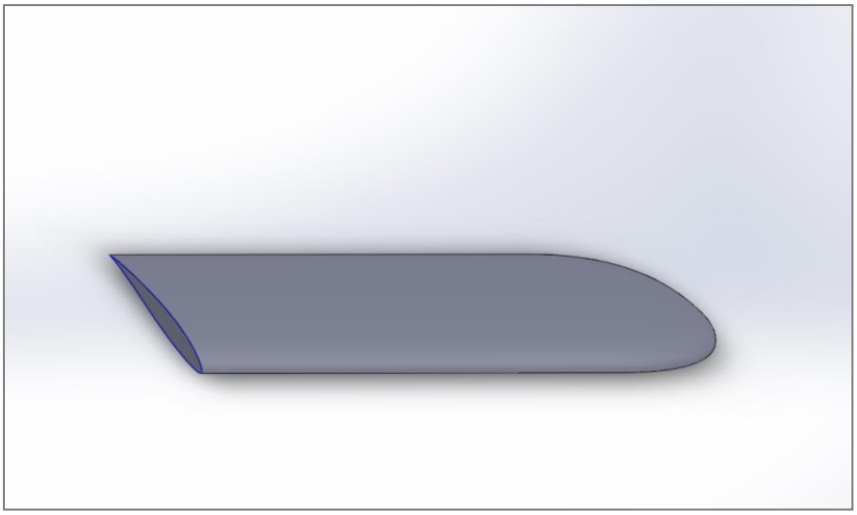

Figure 9. Elliptical geometry generated with SolidWorks.

Regarding the Endplate winglet, some meshing problems were encountered too. Still, in this case a satisfactory model was finally achieved and eventually simulated with ANSYS. Figure 11 and 12 depict the final results.

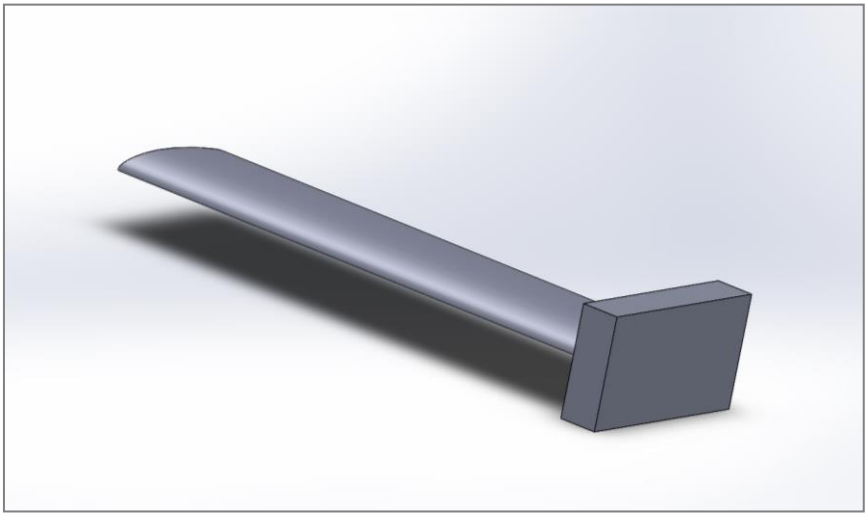

Figure 10. Endplate geometry generated with SolidWorks.

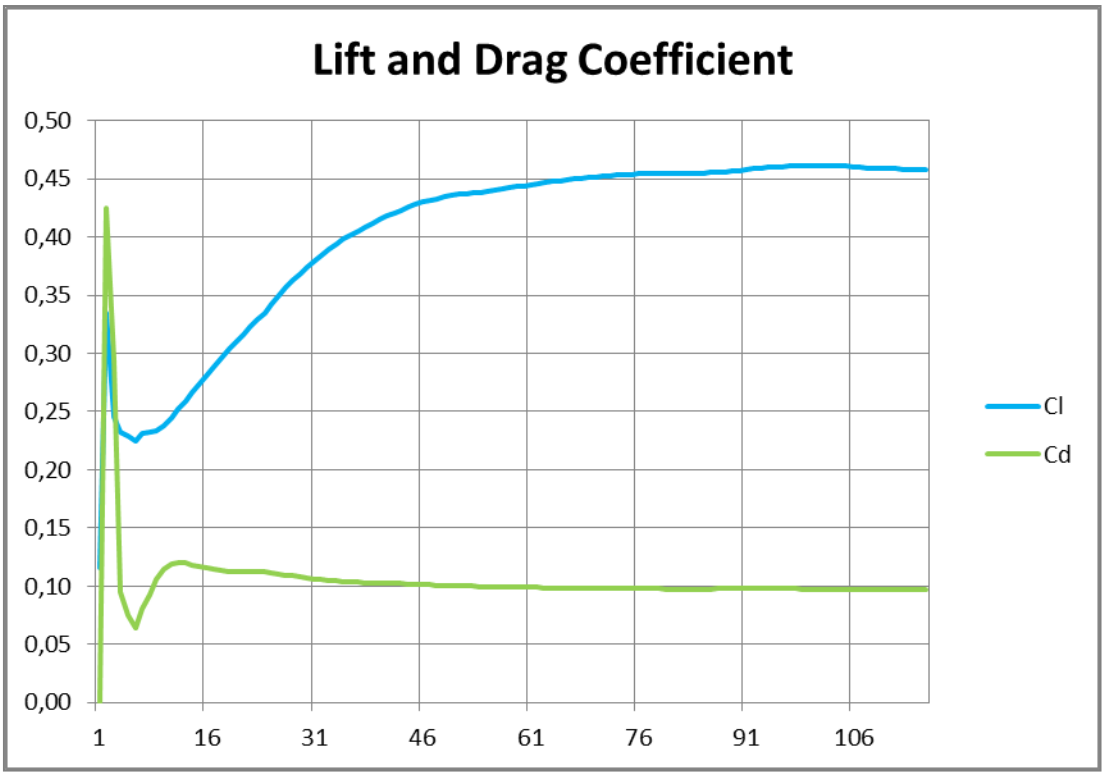

Figure 11. Lift and Drag coefficient evolution during the iteration process.

Lift Coefficient	Drag Coefficient
0,458	0,0973

Figure 12. Lift and Drag Coefficient.

As it can be clearly perceived, even though the lift coefficient had indeed increased, the drag coefficient had done so too. This implied that the final design was not correctly polished, which can easily be deduced from the many singularities present in the simulation. However, it is important to remark that these singularities were originally refined but, due to their curved nature, were not properly meshed by ANSSY mesher, thus forcing a new design without those refinements. Consequently, the Endplate winglet was dismissed too.

Blended winglet without bias tip.

Finally, the last model left to simulate was the blended winglet, both with and without a bias tip. In the case of the blended winglet without bias tip, the geometry did not originate any problems at all, and some of the selected measurements were based on Whitcomb's design.

Still, even though it all seemed to be in favor of this last model, when it came to simulating the geometry, the results showed that, despite an increase of lift coefficient was noticeable, drag did not reduce enough for the design to be considered as valid. However, this implied a great improvement because it headed the process towards what was going to be the final design. The following pictures depict the results obtained once the simulation of the blended winglet without bias tip had been executed.

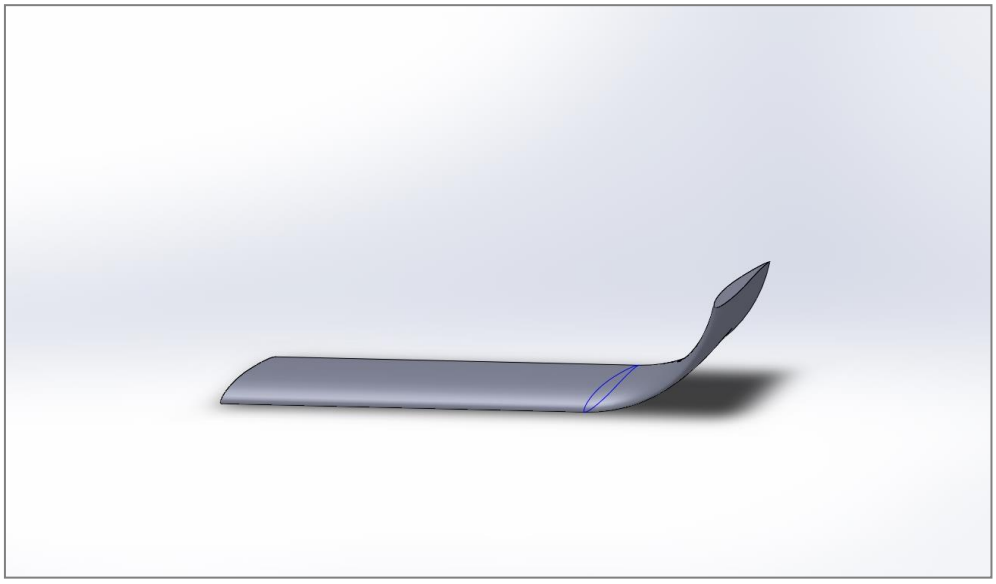

Figure 13. Blended winglet without bias tip geometry.

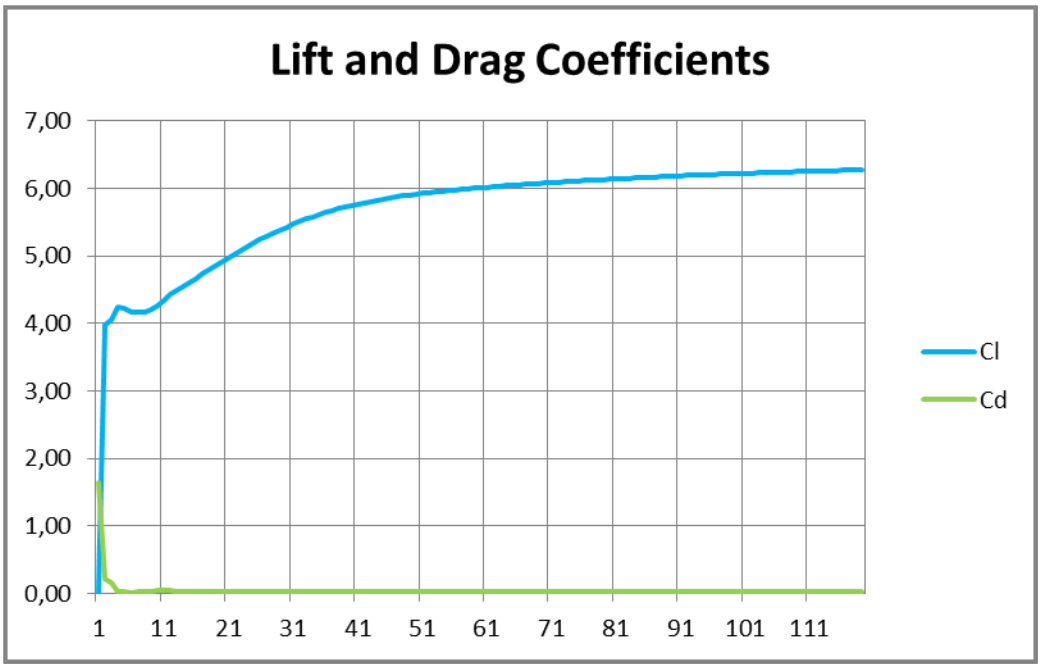

Figure 14. Lift and Drag Coefficient development during the iteration process.

Lift Coefficient	Drag Coefficient
0,627	0,0297

Figure 15. Lift and Drag Coefficients.

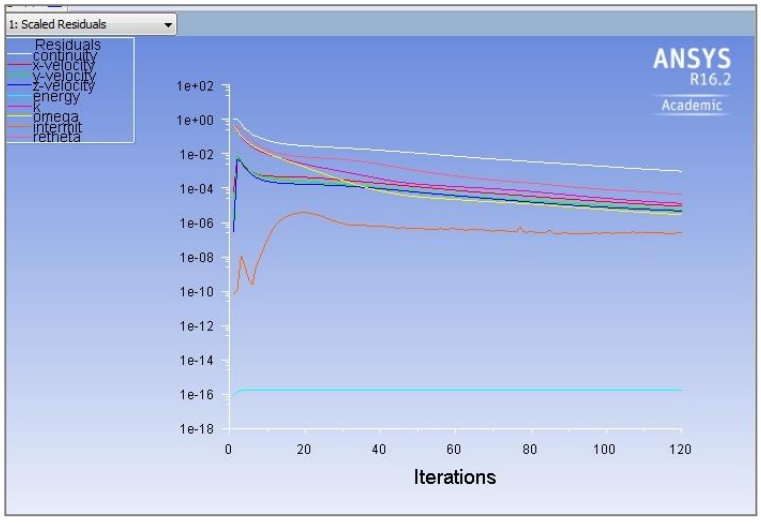

Figure 16. Scaled Residuals after the simulation.

ETSEIB

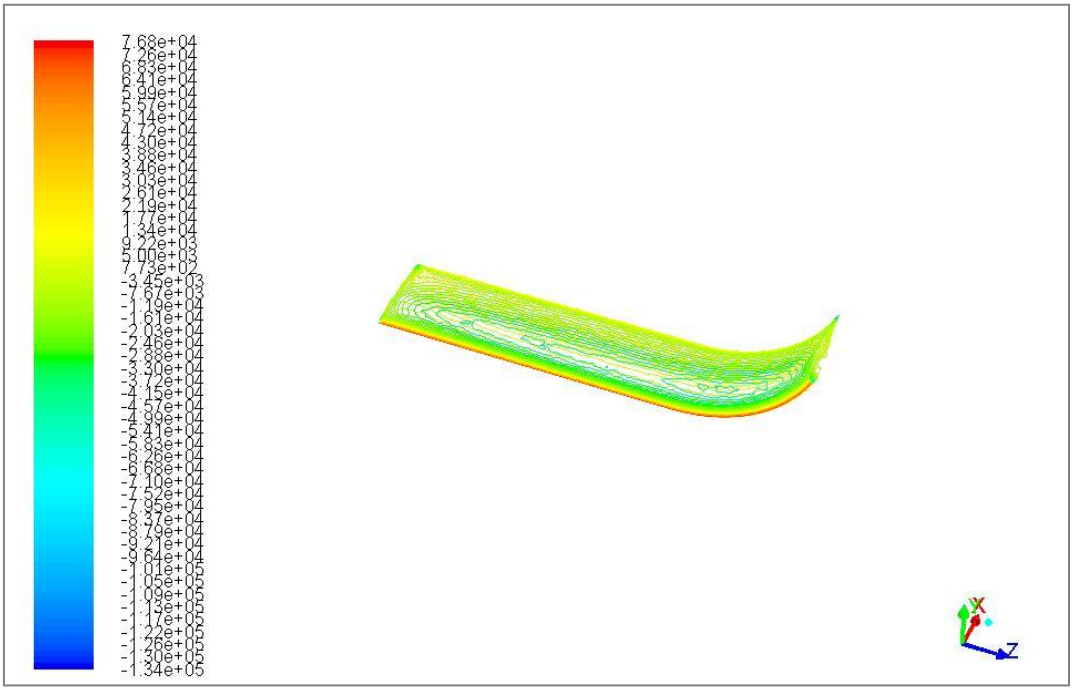

Figure 18. Static pressure distribution of the blended winglet without bias tip.

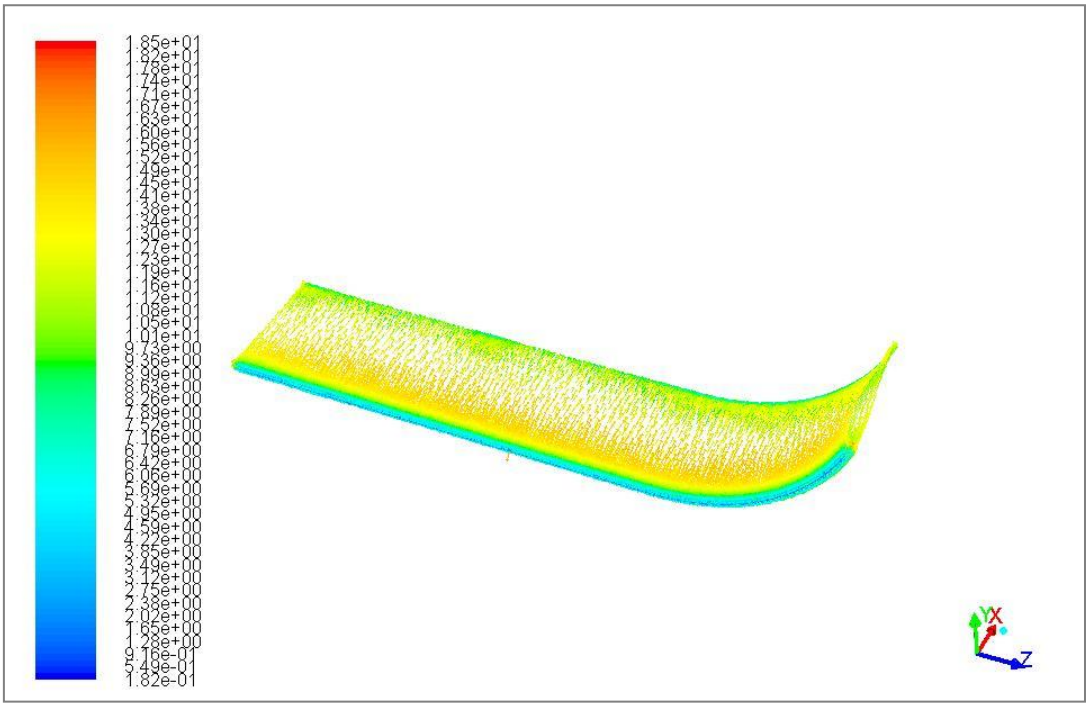

Figure 17. Velocity distribution of the blended winglet without bias tip.

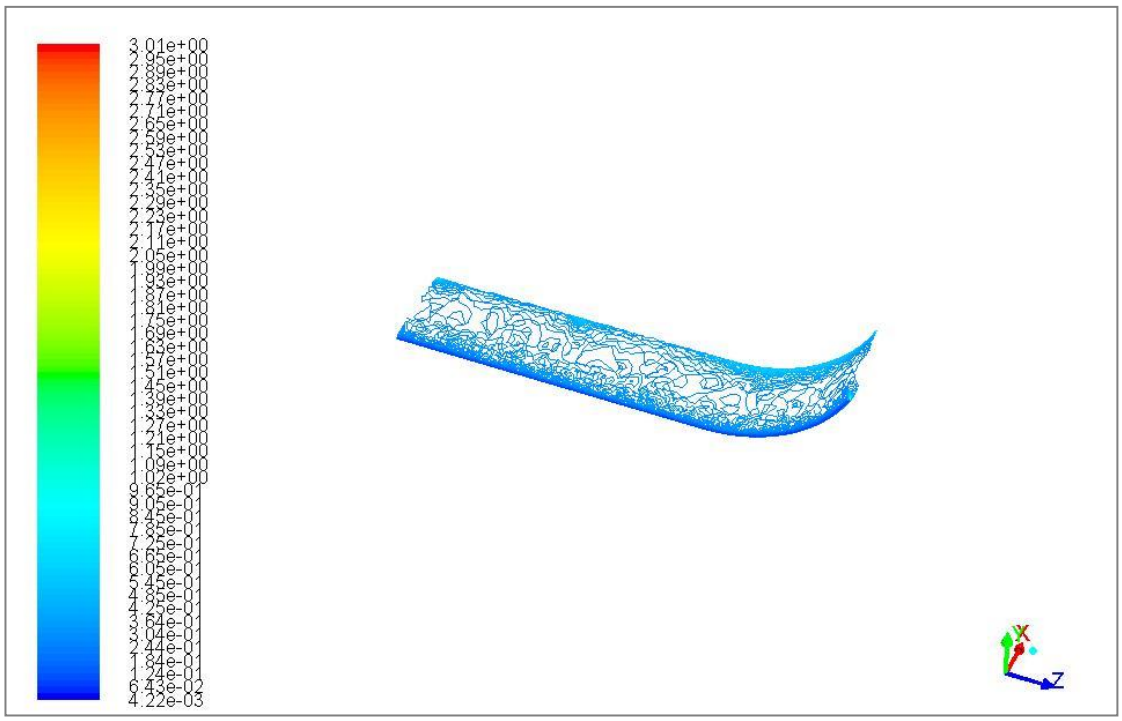

Figure 20. Turbulent Kinetic Energy of the blended winglet without bias tip.

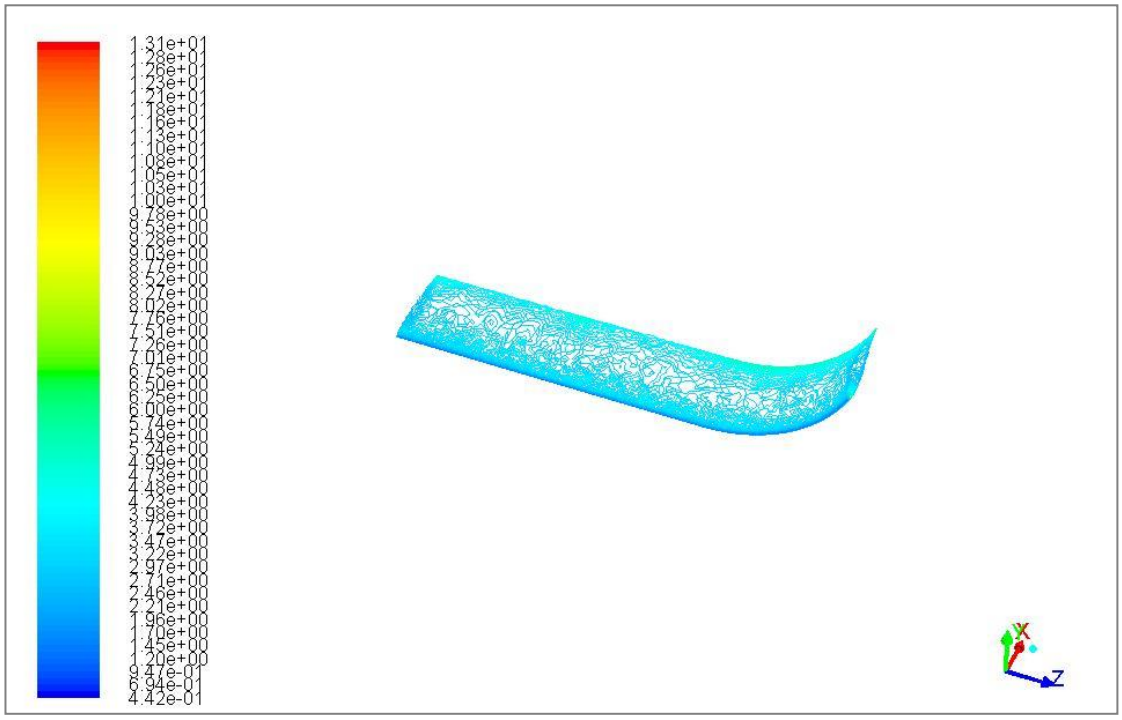

Figure 19. Turbulent Intensity of the blended winglet without bias tip.

Blended winglet with bias tip.

The blended winglet with bias tip model was the final geometry selected to model the winglet that should be attached to the hydrofoil in order to reduce induced drag. The following figures depict some additional data that compliments that which already appears in the main project.

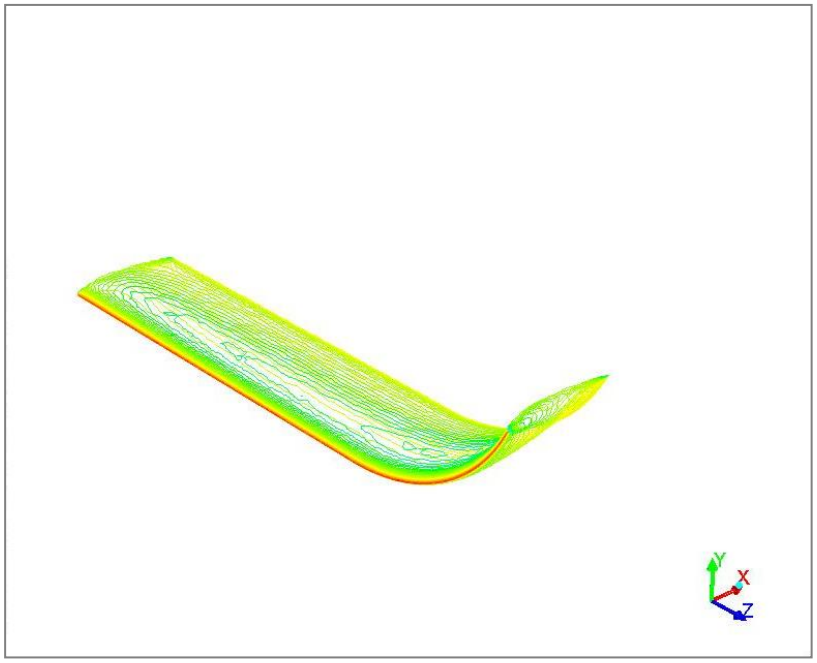

Figure 21. Static pressure distribution of the blended winglet without bias tip.

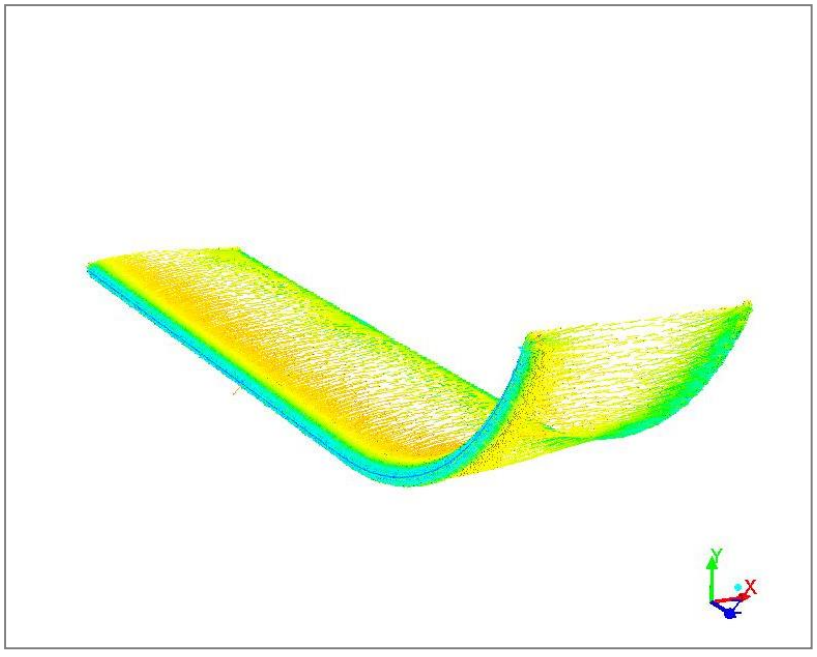

Figure 22. Velocity distribution for the blended winglet without bias tip.

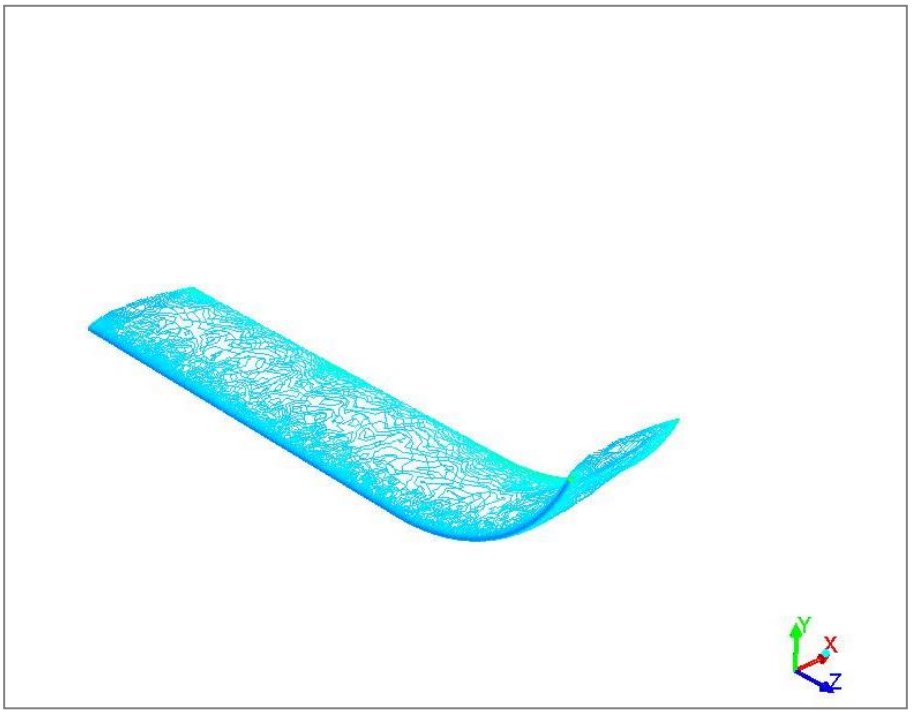

Figure 23. Turbulence Intensity.

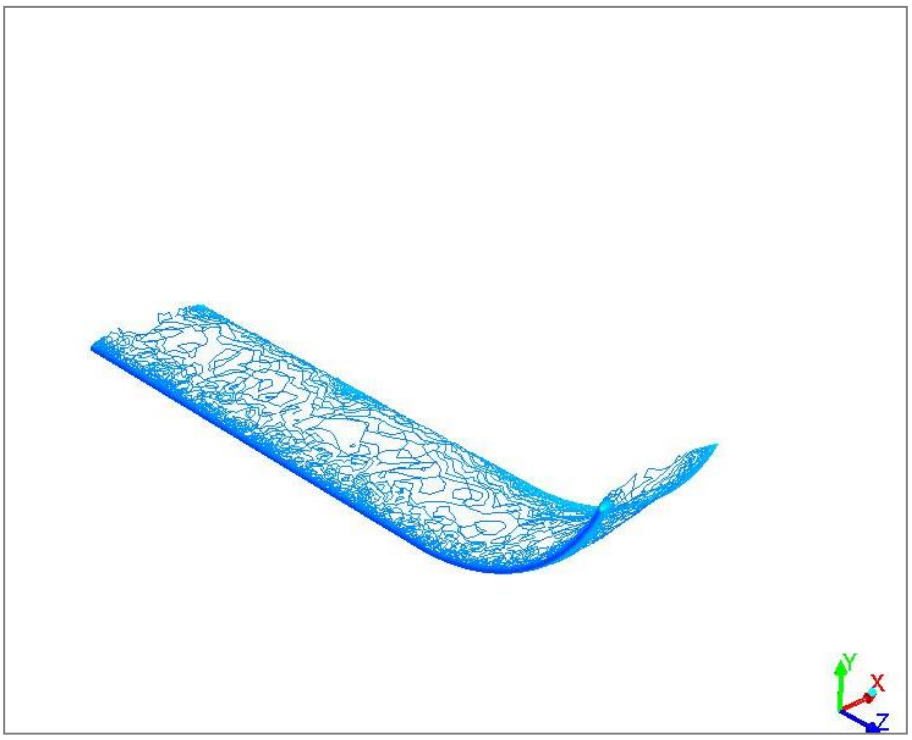

Figure 24. Turbunlence kinetic energy.

Annex B: Model construction, BioFoam, Metaline.

Hypothetical construction of a model.

Besides simulating, it is always useful to build a model. However, given the academic nature of this project the available economic resources are considerably limited, which forces to restrict the construction of the model to a mere hypothesis.

This section acts as a complement to the correspondent section in the memory of the project, which briefly studies the most suitable material for building both the windsurfing board and the hydrofoil. Therefore, this section offers a deeper insight of the properties of the diverse materials available, as well as the main characteristics of the selected material. According to section 11 of the main project, the most used materials for building windsurfing boards, as well as hydrofoils, are Expanded Polystyrene Foam, Fiberglass and Epoxy.

Expanded Polystyrene Foam.

Expanded Polystyrene Foam (EXP) has been a material of choice for over half a century because of its technical versatility, performance and cost effectiveness. It is widely used in many everyday applications where its light weight, strength, durability, thermal insulation and shock absorption characteristics provide economic, high performance products.

Light weight.

EPS is an extremely lightweight material which is not surprising considering it is comprised of 95% air approximately. This characteristic makes it deal for use in packaging as it does not significantly add to the weight of the total product thereby reducing transportation costs. Energy consumption for

transport fuel is also reduced and vehicle emissions minimized – all contributing to lower global warming.

Durability.

The exceptional durability of EPS makes it an effective and reliable protective materials, whose odourless and non-toxic nature make it a good option for windsurfing boards.

Moisture resistance.

EPS is a closed cell material and does not readily absorb water, which is an excellent property for being used for building windsurfing boards. There is no loss of strength in damp conditions, and it is moisture resistant, so the highest hygiene requirements are met, thus not polluting the ocean when practicing the sport. Also, EPS will maintain its shape, size, structure and physical appearance even when subjected to prolonged saturation in water; therefore becoming one of the most resistant materials to the adverse effects of moisture content.

Thermal Properties.

EPS gains its exceptional insulating properties from the established air trapped within its cellular structure. Since it contains no CFCs or any other gas that may leak out, it will not harm the ozone layer or decrease its insulation properties.

Shock absorption.

EPS exhibits excellent shock absorbing characteristics making it one of the first choices for windsurfing boards. Boards are subjected to constant clashes due to water movement, so using shock resistant materials to build them assures that the board will last longer. This durability also guarantees that the board will not be discarded soon, thus forcing companies to build more boards that might end up polluting the environment.

Floating Properties.

The density of EPS is low compared to water, with a normal density range of 11 to 32 kg/m^3 compared to water. The water buoyancy per cubic meter of EPS is determined by subtracting its kg/m^3 density from 1000. The result is the weight in kilograms that a cubic of EPS can support when fully submerged.

Toxicity.

Extensive research programs have been conducted [4] to determine if thermal decomposition products of EPS present a toxicity hazard. The test results have revealed that these decomposition products are less harmful than those of burning wood. Also, gases realeased during combustion are predonminatly carbon monoxide and, to a lesser extent, carbon dioxide, thus deducing that the toxicity of such gases is no greater than that associated with timber[4].

Figure 9 provides a deeper insight on the diverse properties of EPS.

Physical Property	Unit	Class						Test Method
		L	SL	S	M	H	VH	
Nominal Density (kg/m3)		11	13.5	16	19	24	28	N/a
Compressive stress at 10% deformation (min)	kPa	50	70	85	105	135	165	AS2498.3
Cross-breaking strength (min)	kPa	95	135	165	200	260	320	AS2498.4
Rate of water vapour transmission (max) measured parallel to rise at 23°C	µg/m^{2}s	710	630	580	520	460	400	AS2498.5
Dimensional stability of length, width, thickness (max) at 70°C, dry condition 7 days	%	1.0	1.0	1.0	1.0	1.0	1.0	AS2498.6
Thermal resistance (min) at a mean temperature of 25°C (50mm sample)	M^{2}K/W	1	1.13	1.17	1.20	1.25	1.28	AS2464.5 or AS2464.6
Flame propagation characteristics: - median flame duration; max - eighth value; max - median volume retained; - eighth value; min.	 S S % %	 2 3 15 12	 2 3 18 15	 2 3 22 19	 2 3 30 27	 2 3 40 37	 2 3 50 47	AS2122.1

Figure 25. Physical properties of EPS [4].

Fiberglass.

Fiberglass composite material is a stable and inactive material both in usual and aggressive environments (salt solutions, acid, etc.). Tests of chemical stability evidenced that at the impact of weal and concentrated acid, the material preserves all its properties and structure. It is most commonly made of very thin glass filaments (usually only a few micrometres in diameter) that are made by pushing molten glass through superfine holes, and then weaving the strands of glass into a thermoset polymer matrix. It is not glass reinforced plastic as the glass strands are the main component.

Hight strength and stiffness.

Fiberglass has high strength and stiffness due to its Young Modolus, which is higher than its potential rivals in matters of windsurfing boards. Fiberglass needs to be strong in order to be able to withstand the constant, high powered force of the water being imposed on it. It also needs to be stiff, unbreakable and able to withstand the weight of the user of the board.

The matrix that constitutes fiberglass is a continuous material which is usually made of less stiff and weaker material than the reinforcement. It is used to hold the reinforcement together and distribute the load among the reinforcements.

Water proof.

This is a very useful property tht makes it good for the shell windsurfing boards as they spend a lot of time in the ocean. Therefore, the material that is used to build them must not absorb water, or let it in and wet the inner polystyrene of the board. Fiberglass is also chemically resistant to foams of alkaline, which is good considering that the sea is slightly alkaline. This also stops the material from rotting and allowing water in over time.

Light Weight.

Windsurfing boards need to be lightweight so that they are ab le to float as well as support a human body on top of it. This is mostly down to the density of the material. Fiberglass, for instance, has a density of 1900 kg/m^3.

Easy to shape.

Given that fiberglass undergoes plastic deformation, it only breaks via crack propagation when a large force is exerted on it.

Figure 10 provides the general properties of some of the types of fiberglass that exist.

Material	Specific gravity	Tensile strength MPa (ksi)	Compressive strength MPa (ksi)
Polyester resin (Not reinforced)[12]	1.28	55 (7.98)	140 (20.3)
Polyester and Chopped Strand Mat Laminate 30% E-glass[12]	1.4	100 (14.5)	150 (21.8)
Polyester and Woven Rovings Laminate 45% E-glass[12]	1.6	250 (36.3)	150 (21.8)
Polyester and Satin Weave Cloth Laminate 55% E-glass[12]	1.7	300 (43.5)	250 (36.3)
Polyester and Continuous Rovings Laminate 70% E-glass[12]	1.9	800 (116)	350 (50.8)
E-Glass Epoxy composite[13]	1.99	1,770 (257)	
S-Glass Epoxy composite[13]	1.95	2,358 (342)	

Figure 26. General properties of some of the types of fiberglass that exist.

Epoxy Resin.

Finally, it is time to address Epoxy Resin, which was the final choice when selecting the most adequate material to build a model for the windsurfing board and its correspondent hydrofoil.

In any high-tech structural application where strength, stiffness, durability and light weight are required, epoxy resins are seen as the perfect standard of performance for the matrix of the component due to their numerous advantages over other materials like polyester.

For instance:

- Epoxy has better adhesive properties.
- Superior mechanical properties (particularly strength and stiffness).
- Improved resistance to fatigue and micro cracking.
- Reduced degradation from water ingress (diminution of properties due to water penetration).
- Increased resistance to osmosis (surface degradation due to water permeability).

Of all these extremely interesting properties, Fatigue Resistance, Degradation from Water Penetration and Osmosis are the ones that are most appealing to this project's characteristics.

Fatigue Resistance.

The superior ability to withstand cyclic loading is an essential advantage of epoxies vs. polyester resins. This is one of the main reason why epoxies are chosen almost exclusively for watercrafts structures. Figure 11 illustrates the stated comparison, demonstrating the superiority of Epoxy over the first case.

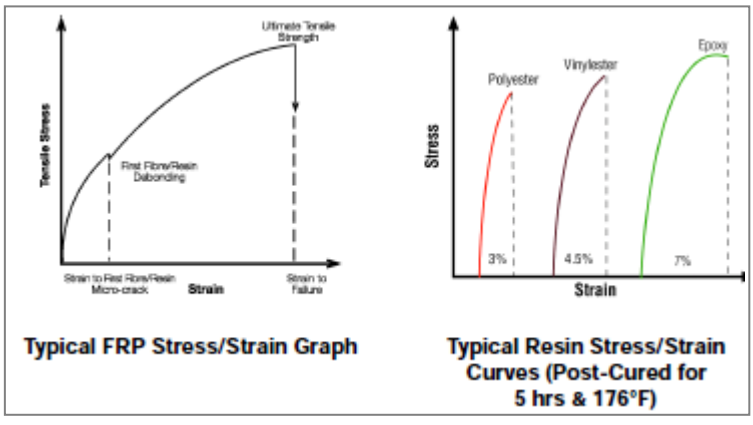

Figure 27. Stress/Strain curves for Epoxy and other materials.

Degradation from Water Penetration.

An important property of any resin, particularly in a marine environment, is its ability to withstand degradation from water penetration. All resins will absorb some moisture, adding to a laminate's weight, but what is more significant is how the absorbed water affects the resin. Polyester is prone to degradation due to the presence of hydrolysable ester groups, while epoxy laminate immersed for the same period will retain around 90% of its original properties.

Osmosis.

To delay the onset osmosis, it is necessary to use a resin that has both a low water transmission rate and a high resistance to attack by water. A polymer chain having epoxy linking in its backbone is substantially better than polyester systems at resisting the effects of water. Figure 12 provides a general overview of some of the main properties of Epoxy.

Mechanical Properties	
Glass transition temperature (Tg)	120 - 130 °C
Tensile strength	85 N/mm²
Tensile Modulus	10,500 N/mm²
Elongation at break	0.8%
Flexural strength	112 N/mm²
Flexural Modulus	10,000 N/mm²
Compressive Strength	190 N/mm²
Coefficient of linear thermal expansion	34 10-6
Water absorption - 24 hours at 23°C	5-10 mg (0.06-0.068%) ISO 62 (1980)
Thermal Properties	
Thermal Shock	2000 cycles (90 sec. at 75 °C, 90 sec. dwell, 90 sec. at 15°C) No effect Should not be subjected to dry-ice or liquid nitrogen.
Smoke Emission	Low Smoke Emission – BS 6853 1999 App. D Clause d.8.4 Result – Ao(on) 8.75, Ao(off) 10.41
Flammability	Class 0 as classified by the current Building Regulations
Thermal Decomposition	350° C
Radioactive Decontamination	BS 4247 Part 1 Test
Decontamination factor (geometric mean)	A5598
Deviation factor	1.25
Ease of decontamination classification	"Excellent"

Figure 28. Properties of Epoxy Resin.

BioFoam.

On a parallel line, this section also deepens into the concept of *BioFoam* and briefly introduces composite plastics, which are biodegradable through composting and whose collective include BioFoam as a constituent.

Composite Plastics.

Compostable Plastics are a new generation of plastics which are biodegradable through composting. They are derived generally from renewable raw materials like starch (e.g. corn, potato, tapioca etc), cellulose, soy protein, lactic acid etc., are not hazardous/toxic in production and decompose back into carbon dioxide, water, biomass etc. when composted. Some compostable plastics may not be derived from renewable materials, but instead derived made from petroleum or made by bacteria through a process of microbial fermentation

Properties.

The compostable resins for the most part mimic plastic properties, and different resins have different properties related to heat resistance, tensile strength, impact resistance, etc. One of the main compostable resins PLA, for instance, has a heat resistance of only 110 F, wheareas other compostable resins can have much higher values.

Biodegradability.

Bioplastics can take different length of times to totally compost, based on the material and are meant to be composted in a commercial composting facility, where higher composting temperatures can be reached and is between 90-180 days. Most existing international standards require biodegradation of 60% within 180 days along with certain other criteria for the resin or product to be called compostable.

Focusing on BioFoam.

BioFoam, from Synbra Technology[5], is a new biodragradable EPS, whose environmentally friendly nature makes it an utterly interesting material to bear in mind when studying the diverse candidates to build a hypothetical model of the windsurfing table and its correspondent hydrofoil.

The main attractiveness of BioFoam is that it is made from plant and vegetable waste, and even though it was originally thought for the packaging industry, in the future it could even replace EPS in some building materials – as in the case of windsurfing boards – given that the raw material from which EPS is made (petroleum) is becoming more and more scarce.

Thefore, BioFoam occupies the leading position in Europe regarding Expandable Polystyrene (EPS) for Sustainable Materials. It is produced from the renewable source PLA, thus presenting a different environmental profile over traditional oil based plastics. Besides its agricultural origin, one of the main characteristics of BioFoam is that after use, it can be remoulded into a new product and it has additional end of life options. It can be completely biodegraded, composed or used for feedstock for recycling. Being "designed for the environment"[5] implies there is no chemical waste, which complies with the principles of environmentally friendly materials.

Energy requirements and CO2 emission for polymers.

As recently highlighted on the Bioplastics markets conference in Guangzou[6], bioplastics use renewable or biogenic carbon as building block. This biogenic carbon is captured from the atmosphere by plants during the growth process and converted into the required raw materials. When the product is being incinerated at the end of its useful life, the biogenic carbon is returned to the atmosphere, thus being cycled in a closed biogenic loop referred to as being "carbon-neutral".

PLA, which is the main raw material of BioFoam, has a different production process than most

polymers. This particular polymer is derived from the production of sugar cane, which is being refined to sugar, then fermented to lactic acid, from which lactide is being made. Lactide is finally polymerized to PLA. Figure 13 depicts the kg of CO_2 emissions to produce one ton polymer of different natures.

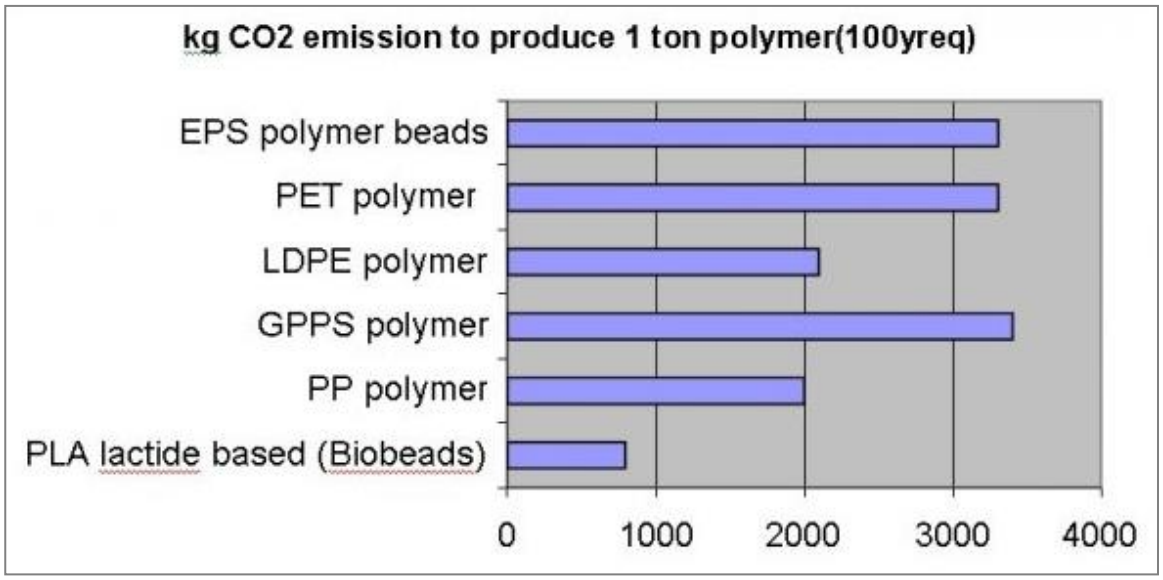

Figure 29. CO_2 emission arising from the production of 1 ton polymer production.

It is noticeable that PLA lactide based materials like BioFoam or many other Composite Plastics, produce less kg of CO_2 emissions, thus causing substantially less harm to the environment.

The most important gain lays in the fact that during the growth of the plants net, CO_2 is absorbed. The sugar cane plant stores CO_2 forming sugar under the influence of sunlight. This energy represents a large part of the energy needed of the end product and does not come from oil, unlike ordinary EPS.

Processing.

The foam expansion process and moulding process for BioFoam is being developed at a rapid pace. The process of moulding is diligently adapted to suit expansion of the raw beads in existing EPS shape, resulting in uniform expanded beads and uniform cell structure. A spherical and uniform series of raw beads in three classes sized 0,6 – 0,7 mm, 0,8 – 1,0 mm, 1,0 – 1,4 mm can be produced to suit

the specific moulding application, as Figure 14 demonstrates.

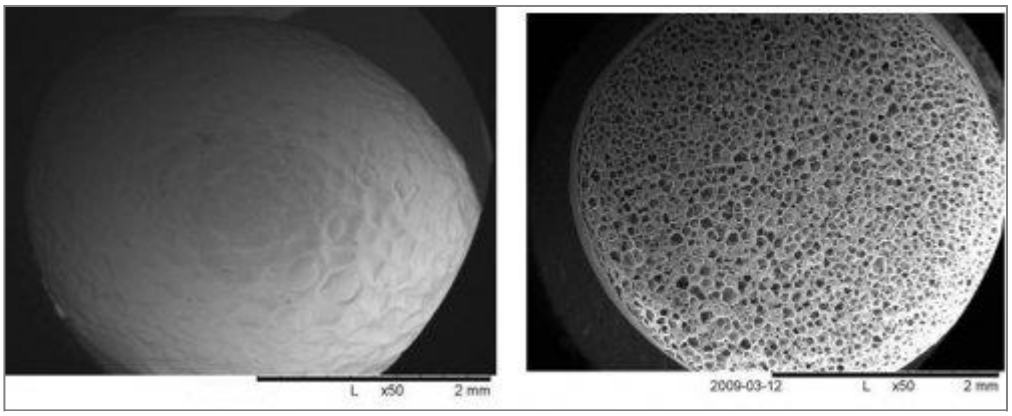

Figure 30. Image of an expanded PLA bead with a closed cell structure and uniform size.

Physical and thermal properties.

The physical properties of BioFoam have been determined (Figure 15) and bear a good resemblance with EPS. The thermal properties are strikingly similar, which as lead to an interest in the cooled transport supplies for medical substances.

		BioFoam		EPS	
property	unit	density	value	density	
thermal conductivity	Mw/Mk	35	34	30	33
compressive strength	kPa	40	200	30	200
C value (drop testing)			2,5		2,4
bending strength	kPa	36	300	30	300
Youngs modulus	Mpa	25	3,2	35	3,2

Figure 31. BioFoam mechanical and thermal properties.

Cavitation Resistance Coatings: Metaline®.

Metaline is a material concept combining the eddiciency and performande of vulcanized tuber coating with the simple processing of epoxy-ceramics with extreme lifetime improvements.

Natural rubber is a proven wear and corrosion protection material. However, with seams that can fail, restricted reparability and its equipment intensive need for field vulcanization, rapid in-situ repairs are not possible. Metaline is an elastomeric materal system that offers a different solution. This new product combines rubber wuality features with a novel cartridge spray process. Using this technique, it is possible to apply sprayable elastomer wear protection coatings directly on site. This product is based on a spectial PUR-Elastomer technology that does not require vulcanization, and the resultsin hydro-dynamically resilient protective coatings, developing an erosion and cavitation resistance are remarkable.

The product.

Metaline is a solvent-free two-component elastomer which adheres to almost any substrate, and its temperature resistance is between -50ºC and +120ºC depending on the relevant application. Also, it cures without any tension and develops in addition to its chemical adhesion a mechanical memory effect. This pulls the coating permanently against the substrate thus counteracting any separation tendency. However, the strength of Metaline lies intis erosion and cavitation resistance, as well as its density and lightweight. It is Abrasion/erosion resistant, permanently elastic, cavitation minimizing, shock absorbing and corrosion resistant.

Figure 14 provides the general properties of Metaline.

	MetaLine 760	MetaLine 785	MetaLine 795
Hardness sprayed /cast on (A.S.T.M. D2240-68)	60 / 65 Shore A	82 / 85 Shore A	95 / 98 Shore A
Density (DIN 53 479)	1.10 g/cm³	1.05 g/cm³	1.05 g/cm³
Tensile strength (A.S.T.M. D412-68)	20 N/mm²	20 N/mm²	24 N/mm²
Tensile Modulus at 100 % elongation (A.S.T.M. D412-68)	6 N/mm²	7 N/mm²	13 N/mm²
Tear resistance (DIN 53 515)	68 N/mm	55 N/mm	68 N/mm
Elongation at break (A.S.T.M. D412-68)	650 %	380 %	275 %
Bashore resilience (DIN 53 512)	63 %	45 %	27 %
Coefficient of thermal conductivity (DIN 52 612)	0.2 W/K·m	0.2 W/K·m	0.2 W/K·m
Dielectric surface resistivity (DIN 53 482)	7 x 10¹⁰ Ohm	7 x 10¹⁰ Ohm	7 x 10¹⁰ Ohm
Dielectric breakdown voltage (DIN 53 841)	> 5 Kv/mm	> 5 Kv/mm	> 5 Kv/mm
Temperature resistance (dry / wet)	+100 °C / +60 °C	+120 °C / +60 °C	+120 °C / +60 °C
Abrasion according to Taber (A.S.T.M. D1-044-73 - Rad H-22, dry, 1 kg, 1.000 U)	n.d.	8.2 mg	10.5 mg
Abrasion (DIN 53 516)	80 mm³	70 mm³	n.d.
Coefficient of static friction (DIN EN ISO 8295)	$\mu(0)$ = approx. 0.7	$\mu(0)$ = approx. 0.6	$\mu(0)$ = approx. 0.2
Solids contents (DIN EN ISO 3251)	100 %	100 %	100 %
Processing time (at 50 °C)	7 minutes	1 minutes	1 minute
Solidification (at 20 °C - dependent on stress)	> 1.5 days	> 1 day	> 1 day
Coverage (theoretically per mm film thickness)	1.20 kg/m²	1.20 kg/m²	1.20 kg/m²

Figure 32. Metaline properties.

References.

[1] F.R. Menter, M.Kuntz, R.Langty, "Ten Years of Industrial Experience with the SST Turbulence Model", (Otterfing, Germany: Begell Hause, Inc.), 2003.

[2] ANSYS Inc., ANSYS Fluent Meshing User's Guide 15.0 Release, (Canonsburg, PA), November 2013.

[3] ANSYS Inc., ANSYS Fluent Modeling and Meshing Guide 15.0 Release, (Canonsburg, PA), November 2013.

[4] Australian Urethane & Styrene, "Expanded Polystyrene (EPS)", (Kings Park, Australia), 2012.

[5] Synbra, BioFoam, "Energy requirements and CO_2 emission for polymers", *http://www.biofoam.nl/*

[6] Metaline, "Elastomeric Spray Corrosion and Repair Materials to Protect Surfaces against Wear, Erosion, Corrosion and Cavitation.